



A wall-coated catalytic capillary microreactor for the direct formation of hydrogen peroxide

Jeck Fei Ng, Yuntong Nie, Gaik Khuan Chuah, Stephan Jaenicke *

Department of Chemistry, National University of Singapore, 3 Science Drive 3, Singapore 117543, Singapore

ARTICLE INFO

Article history:

Received 22 September 2009

Revised 12 November 2009

Accepted 12 November 2009

Available online 19 January 2010

Dedicated to Professor Hideshi Hattori on the occasion of his 70th birthday.

Keywords:

Hydrogen peroxide

Direct formation

Polymer-incarcerated palladium

Capillary microreactor

ABSTRACT

The direct formation of hydrogen peroxide from H_2 and O_2 was successfully carried out in a capillary microreactor at room temperature and atmospheric pressure. A key element in sustaining the activity of the catalyst is the incarceration of the palladium nanoparticles in a cross-linkable amphiphilic polystyrene-based polymer, prepared following the protocol of Kobayashi [R. Akiyama, S. Kobayashi, J. Am. Chem. Soc. 125 (2003) 3412–3413]. The immobilization effectively reduced the leaching of palladium under acidic conditions. Applying the catalyst as a coating on the inner walls of a capillary enabled the sustained production of 1.1% hydrogen peroxide over at least 11 days. The highest catalyst utilization in a 2 mm capillary reactor was $0.54 \text{ mol}_{H_2O_2}/\text{h g}_{Pd}$. When the inner diameter of the reactor capillary was reduced to 530 μm , the rate was enhanced fourfold to $2.28 \text{ mol}_{H_2O_2}/\text{h g}_{Pd}$ corresponding to a turnover frequency of 0.067 s^{-1} .

© 2009 Elsevier Inc. All rights reserved.

1. Introduction

From the view of green chemistry and atom economy, hydrogen peroxide is the best single-oxygen donor, next to molecular oxygen. The oxygen is cleanly transferred, and the only byproduct is water. Applications of hydrogen peroxide in organic synthesis are reviewed in [1]. On a commercial scale, hydrogen peroxide is used as a bleach in the pulp and paper industry, as a disinfectant in the cosmetic and pharmaceutical industry and as an oxidant in water treatment. In highly purified form, it is used for etching and cleaning in the electronics industry. Recently, several propylene oxide plants have come on stream that utilize hydrogen peroxide for the catalytic oxidation of propylene. However, the hydrogen peroxide used by these units is still manufactured by the Riedl-Pfleiderer process via anthraquinone autoxidation (AO) [2,3]. This now over 70-year old process remains the only process used commercially to produce hydrogen peroxide. Because of the complexity of the process, economics of scale dictate the use of big production units. However, this makes it necessary to transport hydrogen peroxide in concentrated form over large distances to the consumers. The transport costs add substantially to the price of the hydrogen peroxide for the end user. Therefore, despite its advantage as a clean oxidant, hydrogen peroxide is still not economically competitive for the production of bulk chemicals or for more widespread use in wastewater treatment [4]. For most applications, relatively

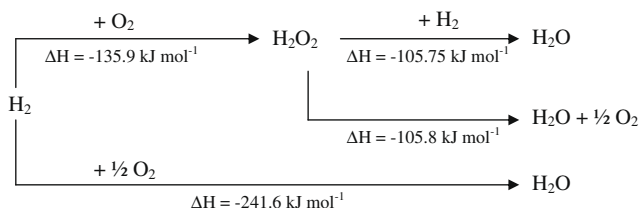
dilute solutions of hydrogen peroxide are adequate and an on-site production would be highly desirable as it would minimize handling and eliminate the need for the transportation of concentrated hydrogen peroxide over long distances.

Extensive studies have therefore been carried out on the direct catalytic formation of hydrogen peroxide from hydrogen and oxygen (**Scheme 1**). The reaction is triphasic, involving a gas (H_2 and O_2), liquid, and solid phase (catalyst). Control of the selectivity of hydrogen peroxide formation and its subsequent decomposition and hydrogenation to water remains a major challenge. In order to achieve a more favorable equilibrium and higher conversion, most reported processes involve extreme operating conditions such as high pressures of 50–96 bar [5–8].

Palladium has been identified as the best catalyst. It has been used in a variety of forms, e.g., as colloids [9–11] or is supported on supports such as silica, titania, and zirconia, or as alloys [12–20] in aqueous or methanolic acid solutions. Using palladium supported on alumina, Choudhary et al. [16] studied the effect of various halide ions and established that the best promoter for hydrogen peroxide formation is the bromide ion. Furthermore, the leaching of palladium from the support was reduced in the presence of phosphoric acid. The nature of the support has a major influence on the selectivity of the catalyst. Edwards et al. [20] observed that the pretreatment of the activated carbon with acetic acid prior to depositing Au/Pd nanoparticles to form the catalyst completely suppressed the reduction of hydrogen peroxide by hydrogen. Using a non-explosive mixture of 3.6% v/v of H_2 and 7% O_2 in CO_2 at a total pressure of 40 bar and at a temperature of

* Corresponding author. Fax: +65 6779 1691.

E-mail address: chmsj@nus.edu.sg (S. Jaenicke).



Scheme 1. Formation of hydrogen peroxide from H_2 and O_2 and competing reactions.

2 °C, these authors obtained a productivity of 0.175 mol $_{\text{H}_2\text{O}_2}$ /h g $_{\text{cat}}$ at a remarkable selectivity of >98%.

An obvious drawback in the formation of hydrogen peroxide from H_2 and O_2 is the very wide explosive regime, 5–96 vol%, in the H_2/O_2 system. To avoid the potential hazards from direct contact between H_2 and O_2 , catalytic membranes [21–23] and a fuel cell design [24,25] have been proposed. Melada et al. [22] studied the continuous formation of hydrogen peroxide over Pd/Pt on carbon-coated membranes. A relatively low hydrogen peroxide concentration of 400 ppm was obtained using O_2 -saturated acidic solutions in the presence of bromide ions and hydrogen, fed in at 3 bar. Another approach is the use of microreactors to achieve the direct formation of hydrogen peroxide. Microreactors mitigate the inherent hazards of a thermal runaway because their large surface to volume ratio allows for highly efficient heat transfer. Furthermore, the free radicals that are needed to sustain the chain reaction during an explosion are efficiently quenched through wall collisions. The volume hold-up in microreactors is also very small. Microreactors are therefore inherently safe. In many cases, higher product yield and purity have been achieved in microreactors than in conventional equipment due to a much higher gas–liquid mass transfer coefficient [26]. Another advantage of these small-scale systems is that they can be built at the point of use, and a simple numbering-out allows for rapid capacity increases. Despite these advantages, there are only a few reports on the use of microreactors for the direct synthesis of hydrogen peroxide. Using a single channel packed-bed microreactor at 20 bar and 50 °C, Voloshin et al. [27–29] obtained hydrogen peroxide as a 1.3 wt% solution. Maehara et al. [30] reduced the total system size by using water electrolysis to generate H_2 and O_2 instead of feeding these gases from gas cylinders. The gases were subsequently passed through a Pd/C-coated stacked microreactor. A relatively modest hydrogen peroxide concentration of 8.3×10^{-3} mol/L (0.028 wt %) was obtained at 10 °C in a 0.1 mol/L solution of HCl with a residence time of 93 s.

We have previously reported on the synthesis of hydrogen peroxide over silica-supported Pd/Pt using two different packed-bed microreactor designs [31]. Experiments with a multi-channel design with multiple parallel channels revealed difficulties in maintaining a constant and uniform two-phase flow through all channels. Because of the high surface tension of the liquid, liquid plugs can form, leading to a much increased pressure drop over the affected channel. In turn, the gas will flow through the other channels and no catalytic reaction can take place in the plugged channel.

Microreactors can be made from a wide range of materials, and a variety of fabrication techniques have been proposed such as LIGA (German: Lithographie–Galvanoplastik–Abformung, translating to lithography, electroforming, and molding), DRIE (Deep Reactive Ion Etching), laser ablation, photolithography, hot embossing, injection moulding, powder blasting, and microlamination [32]. However, all these techniques require special fabrication equipment and skills. Here, we report a simpler, easier, and cheaper design, namely a single-capillary microreactor for the direct formation of hydrogen peroxide. As our earlier investigations indicated that the pressure drop in a packed bed is a major concern, we choose an open channel wall-coated system instead, where the palladium catalyst

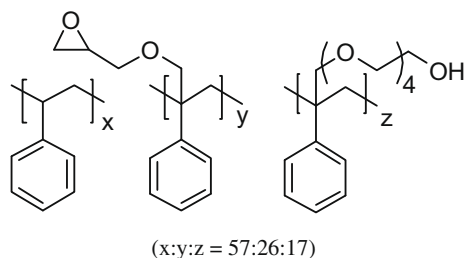


Fig. 1. Copolymer with polystyrene backbone.

nano-particles are immobilized within a thin film of polymer. The polymer-micelle incarceration (PMI) technique developed by Kobayashi and collaborators is used for the immobilization of palladium [33,34]. In this method, an amphiphilic polystyrene-based copolymer (Fig. 1) is induced to form micelles within which a soluble palladium precursor is dissolved. The palladium nanoparticles formed by thermal decomposition are immobilized in the resin by cross-linking. Previous applications of these polymers for micro-encapsulated scandium, ruthenium, and palladium catalysts have demonstrated their resistance to leaching [35–39]. This is attributed to the strong interaction between the π -electrons of the benzene rings in the polystyrene backbone and the vacant orbitals on the metal. Because the liquid phase used for the formation of hydrogen peroxide is normally acidic, the leaching of the metal catalyst is a severe problem. Hence, the polymer-micelle incarceration technique for immobilizing palladium is evaluated as a potential approach to overcome or at least to mitigate the leaching problem.

2. Experimental

2.1. Preparation of polymer-micelle incarcerated palladium (PMI-Pd)

The epoxide-containing polystyrene copolymer was synthesized according to the procedures described in [39]. The exact details of the preparation can be found in the **Supplementary material**. The synthesized copolymer (54 mg) and $\text{Pd}(\text{PPh}_3)_4$ (12 mg) were dissolved in THF (1 mL). Cyclohexane (3 mL) was slowly added to this mixture to form polymer micelles. Glass capillary tubes (ID 2.0 mm; OD 6.5 mm, length 115.0 mm) were washed successively with 1 N NaOH, water, and ethanol, and were filled with the polymer solution. When we attempted to use longer segments of the glass tubes, we observed that it was difficult to evaporate the solvent hexane from the polymer solution to form a uniform coating. Therefore, several shorter pieces were coated on the inside and later combined to provide the necessary length of the reactor. The tubes were mounted horizontally in a fixture in which they could be slowly rotated, and left overnight to precipitate the polymer micelles onto the glass and to allow the solvent to evaporate. After drying, a yellow precipitate covered the inner surface of the tube as a uniform film. The coated glass tubes were washed with hexane, dried, and subjected to heat treatment for 5 h at 150 °C. During this heat treatment, the $\text{Pd}(\text{PPh}_3)_4$ decomposed, forming the palladium metal nanoparticles, and the film changed to black color. The glass tubes were then washed with acetonitrile to remove the liberated triphenylphosphine and any excess (unbound) palladium. Washing was continued until all triphenylphosphine had been washed out as confirmed by the absence of the UV-absorption at 266 nm. To analyze for washed-out palladium, all washings were combined and evaporated to dryness. Concentrated nitric acid (0.1 mL) was added to dissolve the palladium and the solution was made up to 10 mL using deionized water. The washed-out palladium was quantitatively determined by inductively coupled plasma-atomic emission spectroscopy. The amount of palladium catalyst retained in the coating was then calculated as

palladium weighed in at the beginning minus the amount washed out. Typically, more than 90% of the palladium was bound in the polymer matrix. Transmission electron microscopy (TEM) measurements on the fresh and used PMI–Pd catalysts were performed with a JEOL JEM 3010 HRTEM at operated at 300 kV. The samples were mounted by drying a droplet of a suspension containing the ground sample in ethanol onto the copper grid.

2-Aminopropyl derivatized glass surfaces were prepared as described in the literature [33]. The cleaned and washed capillary tubing was filled with a solution of 2-aminopropyl trimethoxysilane in methanol and left at room temperature for 15 h. It was then dried before coating with the polymer micelle solution as described above.

2.2. Direct formation of H_2O_2

Three of the catalyst-coated glass capillary tubes were joined end-to-end with Teflon tubing to form a reactor of 34.5 cm length. All other connections were made with standard HPLC fittings. Hydrogen and oxygen flows were separately controlled via mass flow controllers (MKS). Typical flow rates were 2 and 4 mL/min, respectively. The two gases were mixed using a T-coupling. The liquid phase, a solution of 0.1 N HCl and 0.281 mM KBr in methanol, was then added to the gas stream through the side port of another T-coupling at a rate of 0.5 mL/h via a syringe pump (Harvard Apparatus). The reactor effluent was passed through a gas–liquid separator kept in an ice bath. To avoid the accumulation of dangerous concentrations of hydrogen gas, the outlet of the reactor was diluted with nitrogen to below the explosive limit and removed through a vent line. The system was allowed to stabilize for 2 h at ambient temperature and pressure before the liquid effluent was collected. The hydrogen peroxide formed was quantitatively determined by colorimetry using the $TiOSO_4/H_2SO_4$ reagent [40]. The UV-absorption of the complex was measured at 425 nm. The liquid effluent from the microreactor was collected to test for the leaching of palladium as described above. In order to determine conversion and selectivity, the total gas flow at the inlet and after the reactor was determined with a bubble flow meter. Since water is the only by-product formed, its concentration can then be calculated from a mass balance. The selectivity is given as moles $H_2O_2/(H_2O + H_2O_2)$. The samples of the gas before and after reaction were also collected with a gas tight syringe and the content of H_2 and O_2 was determined with a gas chromatograph (Hewlett-Packard 5890 Plus with thermal conductivity detector; column: molecular sieve 5A, 9' × 1/8"; carrier gas N_2).

2.3. Determination of the length of unit cell

The length of one unit cell refers to the length of one liquid plug plus one gas plug. Due to the slow pumping speed used in the experiment, only one liquid plug was observed within the microreactor at any one time. Subsequent liquid plugs appeared after the first liquid plug has passed through the microreactor. Therefore, the velocity of the liquid plug can be determined from the time required for a liquid plug to pass through the microreactor. The time required for the subsequent liquid plugs to appear was also measured. As the length of the microreactor is known, the distance between two liquid plugs can be estimated.

3. Results and discussion

3.1. Surface Pretreatment

Surface treatment with an amine functionalizing group had been reported to covalently link the PMI–Pd to the glass [33].

The free amino group reacts with the oxirane function of the polymer to form a secondary amine which links the polymer covalently to the capillary wall. However, we found that the presence of the amine linker was incompatible with the reaction conditions to produce hydrogen peroxide. The acidic liquid medium used in the triphasic reaction rapidly hydrolyzed the amine bond and weakened the attachment between the polymer and the glass surface. As a consequence, the palladium-containing film was washed out from the reactor, and the production of hydrogen peroxide at a concentration of 200 mM could only be sustained for 2 days. For subsequent experiments, the PMI catalyst was therefore deposited directly on the surface of the glass capillaries without prior chemical surface functionalization.

3.2. Composition of the solvent system

The composition of the solvent system was varied in order to assess the effect of different modifiers on the direct formation of hydrogen peroxide (Table 1). Initial trials with pure water gave low H_2O_2 yields. Methanol was therefore chosen as the solvent because the solubility of H_2 is three times and that of O_2 eight times higher in methanol than in water [18]. Furthermore, alcoholic hydrogen peroxide would be compatible with the subsequent processes, e.g., in the production of propylene oxide [11–13,26]. Using pure methanol as the solvent, the hydrogen conversion was as high as 47%, but hydrogen peroxide was obtained only with a concentration of 28 mM. After the addition of potassium bromide to the methanol, the concentration increased to 47 mM. Even better results were obtained when the methanol was acidified. Sulfuric acid was tested as it does not cause the specific corrosive effects of halide ions such as pitting and stress corrosion. The achievable hydrogen peroxide concentration increased significantly, from 28 mM to 156 mM. When the methanol was acidified with hydrochloric acid, the final concentration was slightly lower at 107 mM. A further increase in the hydrogen peroxide concentration was obtained when potassium bromide was added to the acidified methanol. Using $MeOH/H_2SO_4/KBr$ as the solvent doubled the hydrogen peroxide concentration to 278 mM, while in the $MeOH/HCl/KBr$ system, the hydrogen peroxide obtained had a concentration of 326 mM. With the latter liquid phase composition, the productivity of the hydrogen peroxide at 0.54 mol/h g_{Pd} is about 10 times that observed in pure methanol. Both the hydrogen and halide ions (Cl^- and Br^-) are known to promote the hydrogen peroxide yield by inhibiting its hydrogenation and decomposition [10,14,41]. The halide ions presumably block the active sites (consisting of ensembles of metal atoms) for the dissociation of the O–O bond. This is reflected in the dramatic increase in the hydrogen peroxide selectivity from 0.65% without additives to 77% in the system with H_2SO_4 and Br^- , which is the result of a largely decreased H_2 conversion (from 47% to only 3.9%). The observed selectivities are comparable to those observed in a batch reactor under 6 bar total pressure (see data under Supplementary material, Table S-1).

Table 1
Comparison of different solvent systems for the synthesis of hydrogen peroxide.

Solvent system	Conc. of H_2O_2 (mM)	Productivity (mol/h g _{Pd})	H_2 conv. (%)	Selectivity ^a (%)
MeOH	28	0.05	47	0.65
MeOH/KBr	47	0.08	36	1.4
MeOH/HCl	107	0.18	nd	nd
MeOH/ H_2SO_4	156	0.26	20	8.7
MeOH/ H_2SO_4 /KBr	278	0.46	3.9	77
MeOH/HCl/KBr	326	0.54	nd	nd

Reaction conditions: Pd: 0.30 mg; O_2 : 4 mL/min, H_2 : 2 mL/min; liquid rate: 0.5 mL/h, 0.1 N H^+ and 0.281 mM KBr (aq).

^a Selectivity to H_2O_2 ; nd = not determined.

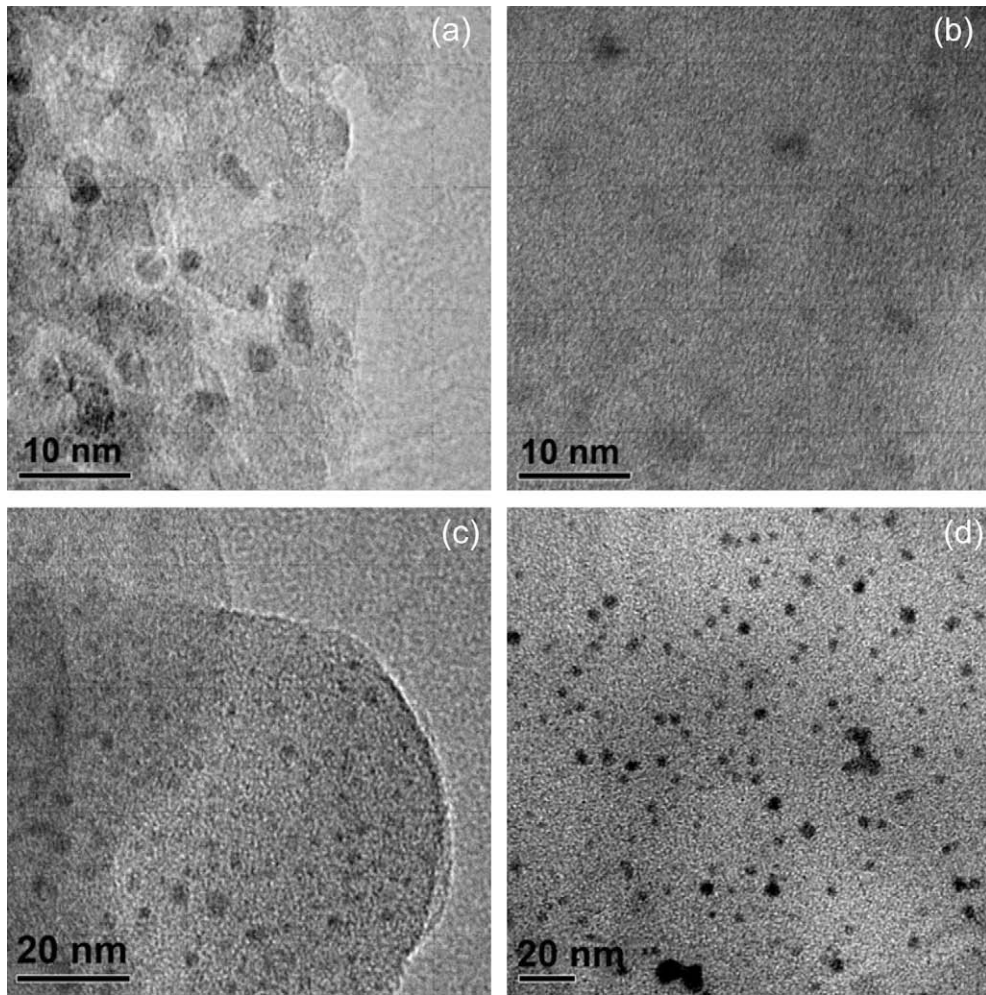


Fig. 2. TEM images for fresh PMI catalysts with (a) 1 wt%, (b) 2 wt%, (c) 4 wt% Pd and (d) 2 wt% PMI–Pd after reaction.

3.3. Influence of catalyst loading

Different palladium loadings into the polymer were achieved by varying the amount of $\text{Pd}(\text{PPh}_3)_4$ in the micelle precursor. Representative TEM micrographs of the resulting PMI–Pd catalysts are shown in Fig. 2. The palladium clusters, represented by the black dots, are well distributed throughout the polymer support. The clusters had a relatively uniform particle size around 2.5, 2.7, and 3.6 nm for 1, 2, and 4 wt% Pd loading, respectively (Table 2). Comparing their activity, the productivity of hydrogen peroxide normalized to the amount of palladium increased from 0.25 to 0.34 mol/h g_{Pd} as the loading increased from 1 to 2 wt%. However, the productivity became lower when the palladium loading was further increased to 4 wt%. While the decrease in activity may be related to the bigger particle size and consequently lower metal dispersion at the higher metal loading, the initial increase appears

to indicate a size effect similar to that observed by Edwards et al. [20]: the activity of the nanoparticles for H_2O_2 formation is optimum at a certain size, but decreases for even smaller particles, over which water formation becomes favored.

Several microreactors were prepared with polymer films containing palladium at a concentration of 2 wt% with respect to the polymer. The amount of catalyst in the reactor was increased by increasing the film thickness through applying multiple coats of the polymer. The concentration of the hydrogen peroxide generated in the microreactor increased linearly from 123 to 254 mM as the catalyst amount increased from 0.19 to 0.35 mg Pd (Table 3). However, the productivity normalized to the amount of catalyst remained essentially constant, varying only slightly from 0.32 to 0.36 mol/h g_{Pd}. This shows that the polymer film was well penetrated by the reactants so that all the encapsulated metal particles were readily accessible for the reaction. Furthermore, the decom-

Table 2
Effect of palladium concentration in the polymer film.

Pd loading (wt%)	Coated Pd (mg)	TEM particle size (nm)	Conc. of H_2O_2 (mM)	Productivity of H_2O_2 (mol/h g _{Pd})
1	0.14	2.5	71.2	0.25
2	0.37	2.7	254	0.34
4	0.59	3.6	293	0.25

Reaction conditions: O₂: 4 mL/min; H₂: 2 mL/min, liquid (MeOH/HCl/KBr): 0.5 mL/h.

Table 3
Influence of palladium loading varied by repeated coating with PMI–2% Pd.

Amount of Pd (mg)	Conc. of H_2O_2 (mM)	Productivity of H_2O_2 (mol/h g _{Pd})
0.19	123	0.32
0.28	207	0.36
0.35	254	0.34

Reaction conditions: O₂: 4 mL/min; H₂: 2 mL/min, liquid (MeOH/HCl/KBr): 0.5 mL/h.

position of hydrogen peroxide was not significant even at the highest loading of catalyst.

3.4. Flow rate of the liquid phase

The flow rate of the liquid plays an important role in the mass transfer within the microreactor. In a 2-mm ID capillary, increasing the liquid feed rate from 0.2 to 1.0 mL/h resulted in an increase in the productivity of hydrogen peroxide from 0.24 to 0.46 mol/h g_{Pd} (Table 4). However, the hydrogen peroxide concentration decreased from 409 mM to 160 mM due to dilution by a larger volume of liquid. Bercic and Pintar [42] found that the gas–liquid mass transfer in a methane/water system under Taylor flow conditions is well described by the relation

$$K_{La} = \frac{\alpha u^\beta}{((1 - \varepsilon_g)L_{UC})^\gamma} \quad (1)$$

In this equation α , β , and γ are constants, and L_{UC} is the length of one “unit cell”, i.e., of one gas bubble and the liquid plug separating it from the next gas bubble, ε_g is the volume fraction of the gas bubbles, and u is the flow velocity of the unit cell. Inspection of this equation shows that an increase of the flow velocity u or a decrease of the unit cell length L_{UC} will have the strongest impact on the mass transfer coefficient K_{La} . The numerical value for exponent γ in our experiments was calculated to be 0.56.

The flow velocity u remains essentially the same if the liquid feed rate is varied at constant gas flow rate because under our experimental conditions, the volume flow rate of the gas is very much higher than that of the liquid. Therefore, the main parameter affected by a change in liquid feed rate is the length of the unit cell. At a higher liquid feed rate, the length of the unit cell becomes

Table 4
Effect of liquid pumping speed in a 2-mm ID capillary reactor.

Pumping speed (mL/h)	Conc. of H ₂ O ₂ (mM)	Productivity of H ₂ O ₂ (mol/h g _{Pd})
0.2	409	0.24
0.5	254	0.34
1.0	160	0.46

Reaction conditions: Pd: 0.35 mg; O₂: 4 mL/min; H₂: 2 mL/min, liquid (MeOH/HCl/KBr): 0.5 mL/h.

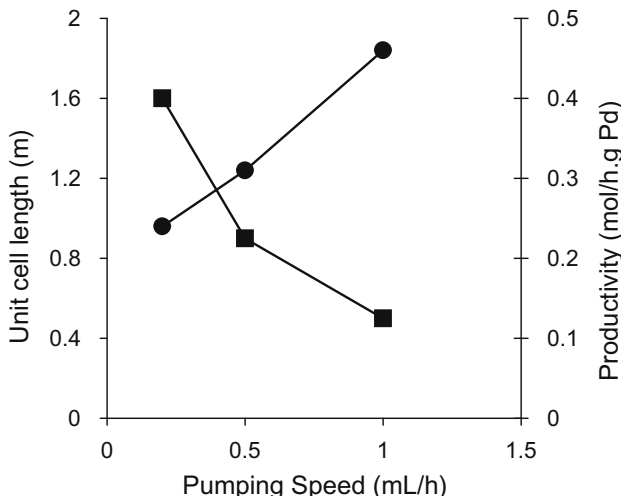


Fig. 3. Dependence of the unit cell length (■) and productivity (●) of H₂O₂ on pumping speed. Reaction conditions: Pd: 0.35 mg; O₂: 4 mL/min; H₂: 2 mL/min, liquid (MeOH/HCl/KBr): 0.5 mL/h.

shorter as more liquid plugs are introduced into the channel per unit time. The shorter unit cell length increases the gas–liquid mass transfer and therefore leads to higher hydrogen peroxide productivity. In Fig. 3 the estimated unit cell length and productivity of hydrogen peroxide are plotted against different liquid feed rates. The results are in good agreement with Eq. (1).

3.5. Influence of microreactor diameter

According to Eq. (1), the mass transfer can also be improved by increasing the flow velocity u of the unit cell. Higher velocity of the unit cell is achieved by maintaining a constant gas and liquid flow rate and decreasing the inner diameter of the reactor at the same time. The results in Table 5 show that the productivity of hydrogen peroxide increased from 0.34 to 2.28 mol/h g_{Pd} when the reaction was run in narrower capillaries. The productivity per unit palladium obtained with a microreactor of 0.53 mm diameter was about six times higher than in one with 2 mm inner diameter. These results clearly confirm that a smaller diameter resulted in a higher velocity of the unit cell and therefore a better liquid–gas mass transfer. However, the concentration of the hydrogen peroxide was lower for the smaller diameter reactor. This is due to the significantly smaller amounts of catalyst-coated on the wall of the narrower capillary. The amount of catalyst deposited onto the walls of the capillary depends on the volume of the solution from which the catalyst was deposited. It will therefore scale with r^2 (r is the radius of the capillary) if a constant number of impregnation steps is used.

3.6. Varying gas ratios and secondary reactions

Scheme 1 shows that except for the decomposition of hydrogen, all other side reactions involve hydrogen. Therefore, it is crucial to optimize the ratio of the O₂:H₂ for maximum formation of hydrogen peroxide. When the amount of hydrogen is stoichiometric (1:1) or higher than that of oxygen (2:1), the formation of hydrogen peroxide is four to seventeen times lower as compared to that for a H₂:O₂ ratio of 1:2 (Table 6). An excess of hydrogen favors the subsequent hydrogenation of hydrogen peroxide to water. Therefore, a moderate oxygen excess is essential to suppress the reduction reactions. The H₂:O₂ ratio of 1:2 was established as close to the economic optimum.

To investigate the secondary reactions that hydrogen peroxide undergoes in the microreactor, hydrogen peroxide at a concentra-

Table 5
Hydrogen peroxide production in different capillary tubes.

Inner diameter (mm)	Coated Pd (mg)	Conc. of H ₂ O ₂ (mM)	Productivity of H ₂ O ₂ (mol/h g _{Pd})
2.00	0.37	254	0.34
1.00	0.12	144	0.61
0.53	0.02	81.7	2.28

Reaction conditions: O₂: 4 mL/min; H₂: 2 mL/min, liquid (MeOH/HCl/KBr): 0.5 mL/h.

Table 6
Variation of H₂:O₂ gas ratio on hydrogen peroxide formation.

Gas ratio (H ₂ :O ₂)	Conc. of H ₂ O ₂ (mM)	Productivity of H ₂ O ₂ (mol/h g _{Pd})
1:2	254	0.34
1:1	58.8	0.08
2:1	17.1	0.02

Reaction conditions: Pd: 0.35 mg; O₂: 4 mL/min; H₂: 2 mL/min, liquid (MeOH/HCl/KBr): 0.5 mL/h.

tion of 200 mM was added to the liquid feed. The hydrogen peroxide concentration in the product stream was measured as a function of the gas phase composition (Table 7). In the absence of hydrogen, the final concentration of hydrogen peroxide remained unchanged. Hence, the catalytic decomposition of hydrogen peroxide was negligible within the short retention time of about 7–8 s in the microreactor. A very significant decrease in hydrogen peroxide concentration was observed in the presence of hydrogen gas. In a He and H₂ (2:1) gas mixture, almost half of the initial hydrogen peroxide was reduced to water, and the hydrogen peroxide concentration decreased from 200 mM to 121 mM. Using our standard synthesis gas mixture of H₂ and O₂ in the ratio of 1:2, the decrease in hydrogen peroxide concentration was smaller, from 200 mM to 165 mM. This was the same concentration that could be obtained with this reactor in the synthesis mode. Obviously, under these conditions, the formation of hydrogen peroxide occurs, but at a lower rate than the reduction of hydrogen peroxide. The final value, 165 mM, is the steady-state concentration between formation and decomposition reactions. We conclude that the main secondary reaction within our microreactor system is the reduction of hydrogen peroxide by hydrogen rather than its decomposition. Our results confirm earlier observations by Han and Lunsford [10] who had shown that under batch conditions, hydrogen peroxide was stable in the presence of O₂ but was readily reduced to water by H₂.

3.7. Lifetime of the catalyst in the microreactor

The long-term behavior of the microreactor for the continuous production of hydrogen peroxide was investigated (Fig. 4). A

hydrogen peroxide productivity rate of 0.34–0.35 mol/h g_{Pd} was sustained over the first 3 days at a daily operation time of 10 h (for safety reasons, the reactor was only operated in the presence of an operator). The productivity decreased over the next 3 days to stabilize at a constant value of 0.27 mol/h g_{Pd}, which is 77% of the initial activity. The productivity was maintained at this level until the experiment was terminated after another 5 days. The concentration of hydrogen peroxide obtained during the period of highest productivity was 0.9 wt%.

The observed decrease in activity between day 4 and day 6 can be attributed to a loss of palladium from the microreactor. This may be palladium particles which are not tightly incarcerated in the polymer and can be easily removed by the acidic liquid phase. Indeed, no further decrease in hydrogen peroxide productivity was observed with continued operation of the microreactor after this time. A control experiment, using an acid- and halogen-free solution of methanol in water as the liquid phase, showed that the amount of palladium in the reactor effluent was below detection limit. The palladium content in the film was analyzed by ICP-AES after the run and was found to be 10% lower than that in the fresh film. This loss in palladium can account for half of the observed decline in productivity. Another contributing factor is the formation of bigger palladium particles and agglomeration of palladium clusters. Transmission electron micrographs of the polymer film after the reaction (Fig. 2d) showed the presence of palladium crystallites with a diameter of up to 4.8 nm, in addition to many small particles that were similar in size or even smaller than the 2.7 nm particles in the as-synthesized film (Fig. 2b). The growth of bigger palladium particles at the expense of smaller ones (Ostwald ripening) will result in lower catalyst dispersion which adequately explains the observed reduction in activity up to day 6. The stable hydrogen peroxide productivity obtained thereafter suggests that the tightly bound PMI-Pd crystallites were stable toward leaching and particle growth.

4. Conclusions

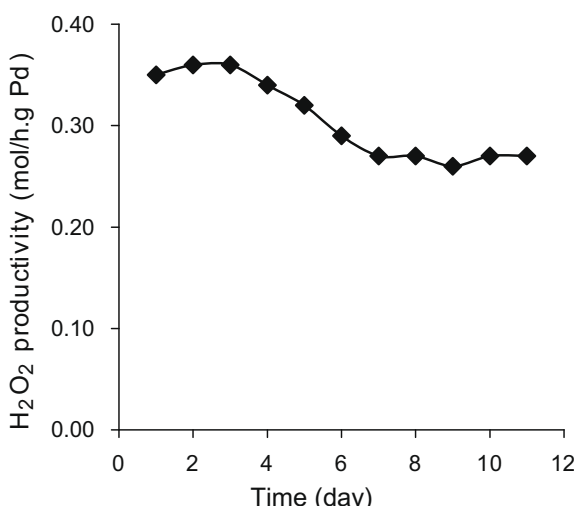
The catalytic capillary microreactor was shown to be a suitable approach for the intrinsically safe *in situ* generation of hydrogen peroxide from the elements. Over a wall-coated Pd nano-particle catalyst, this reaction takes place under mild conditions, i.e., room temperature and atmospheric pressure, without dilution by an inert gas. A moderate excess of oxygen in the feed stream over the stoichiometric 1:1 ratio for O₂:H₂ is necessary to suppress the catalytic reduction of the formed hydrogen peroxide to water. A two-fold oxygen excess was identified as close to the economic optimum.

The immobilization of palladium from a soluble precursor using the PMI method resulted in uniform palladium nanoparticles of 2.5–3.6 nm diameter for palladium loadings of 1–4 wt%. The presence of bromine and hydrogen ions in the solvent system is essential for achieving high productivity of hydrogen peroxide. Despite the corrosive conditions, the PMI catalyst showed little leaching. The long-time stability of the catalyst could be demonstrated during the continuous production of hydrogen peroxide for 11 days. Using a 2-mm ID microreactor coated with PMI-Pd, a maximum concentration of 1.4 wt% of H₂O₂ corresponding to a turnover frequency of 0.54 mol_{H2O2}/h g_{Pd} was obtained in continuous operation.

Acknowledgment

We thank the National University of Singapore for financial support under Grant R-143-000-374-112 and for the award of a research scholarship to J.F.N.

Fig. 4. Productivity of hydrogen peroxide as a function of time. Reaction condition: Pd: 0.283 mg; O₂: 4 mL/min; H₂: 2 mL/min, liquid (MeOH/HCl/KBr): 0.5 mL/h.



Appendix A. Supplementary material

Supplementary data associated with this article can be found, in the online version, at doi:10.1016/j.jcat.2009.11.015.

References

- [1] G. Goor, in: G. Strukul (Ed.), *Catalytic Oxidations with Hydrogen Peroxide as Oxidant*, Kluwer Academic, Norwell, MA, 1992, p. 13.
- [2] J.M. Campos-Martin, G. Blanco-Brieva, J.L.G. Fierro, *Angew. Chem. Int. Ed.* 45 (2006) 6962.
- [3] W.T. Hess, in: J.I. Kroschwitz, M. Howe-Grant (Eds.), *Kirk-Othmer Encyclopedia of Chemical Technology*, vol. 13, 4th ed., Wiley, New York, 1995, p. 961.
- [4] C. Samanta, V.R. Choudhary, *Catal. Commun.* 8 (2007) 73.
- [5] S.N. Gandhi, R.T. Sprague, L. Lin, M. Sangalli, K.M. Vande Bussche, R.A. Janicki, A.R. Oroskar, L.T. Nameth, K.S. Crosby, P. Palmese, US Patent 7 442 283, 2008.
- [6] B. Le-Khac, US Patent 7 357 909, 2008.
- [7] T. Haas, R. Jahn, US Patent 7 364 718, 2008.
- [8] U. Mueller, O. Metelkina, H. Junicke, T. Butz, O.M. Yaghi, US Patent 7 179 765, 2007.
- [9] S. Chinta, J.H. Lunsford, *J. Catal.* 225 (2004) 249.
- [10] Y.F. Han, J.H. Lunsford, *J. Catal.* 230 (2005) 313.
- [11] Y.F. Han, J.H. Lunsford, *Catal. Lett.* 99 (2005) 13.
- [12] Q. Liu, J.C. Bauer, R.E. Schaak, J.H. Lunsford, *Appl. Catal. A* 339 (2008) 130.
- [13] V.V. Krishnan, A.G. Dokoutchaev, M.E. Thompson, *J. Catal.* 196 (2000) 366.
- [14] V.R. Choudhary, P. Jana, *Appl. Catal. A* 352 (2009) 35.
- [15] V.R. Choudhary, P. Jana, *Catal. Commun.* 9 (2008) 2371.
- [16] V.R. Choudhary, Y.V. Ingole, C. Samanta, P. Jana, *Ind. Eng. Chem. Res.* 46 (2007) 8566.
- [17] E.N. Ntainjuam, J.K. Edwards, A.F. Carley, J.A. Lopez-Sanchez, J.A. Moulijn, A.A. Herzing, C.J. Kiely, G.J. Hutchings, *Green Chem.* 10 (2008) 1162.
- [18] Q. Liu, J.C. Bauer, R.E. Schaak, J.H. Lunsford, *Angew. Chem. Int. Ed.* 47 (2008) 6221.
- [19] T. Ishihara, Y. Ohura, S. Yoshida, Y. Hata, H. Nishiguchi, Y. Takita, *Appl. Catal. A* 291 (2005) 215.
- [20] J.K. Edwards, B. Solsona, E. Ntainjuam, A.F. Carley, A.A. Herzing, C.J. Kiely, G.J. Hutchings, *Science* 323 (2009) 1037.
- [21] V.R. Choudhary, A.G. Gaikwad, S.D. Sansare, *Angew. Chem. Int. Ed.* 40 (2001) 1776.
- [22] S. Melada, F. Pinna, G. Strukul, S. Perathoner, G. Centi, *J. Catal.* 235 (2005) 241.
- [23] S. Melada, F. Pinna, G. Strukul, S. Perathoner, G. Centi, *J. Catal.* 237 (2006) 213.
- [24] I. Yamanaka, T. Onizawa, S. Takenaka, K. Otsuka, *Angew. Chem. Int. Ed.* 42 (2003) 3653.
- [25] I. Yamanaka, *Catal. Surveys Asia* 12 (2008) 78.
- [26] S.J. Haswell, P. Watts, *Green Chem.* 5 (2003) 240.
- [27] Y. Voloshin, R. Halder, A. Lawal, *Catal. Today* 125 (2007) 40.
- [28] Y. Voloshin, J. Mangano, A. Lawal, *Ind. Eng. Chem. Res.* 47 (2008) 8119.
- [29] Y. Voloshin, A. Lawal, *Appl. Catal. A* 353 (2009) 9.
- [30] S. Maebara, M. Taneda, K. Kusakabe, *Chem. Eng. Res. Des.* 86 (2008) 410.
- [31] X. Wang, Y. Nie, J.L.C. Lee, S. Jaenicke, *Appl. Catal. A* 317 (2007) 258.
- [32] W. Ehrfeld, V. Hessel, H. Löwe, *Microreactors: New Technology for Modern Chemistry*, Wiley-VCH, Weinheim, 2000, p. 1.
- [33] J. Kobayashi, Y. Mori, K. Okamoto, R. Akiyama, M. Ueno, T. Kitamori, S. Kobayashi, *Science* 304 (2004) 1305.
- [34] R. Akiyama, S. Kobayashi, *Chem. Rev.* 109 (2009) 594.
- [35] R. Akiyama, S. Kobayashi, *J. Am. Chem. Soc.* 125 (2003) 3412.
- [36] K. Okamoto, R. Akiyama, S. Kobayashi, *J. Org. Chem.* 69 (2004) 2871.
- [37] K. Okamoto, R. Akiyama, S. Kobayashi, *Org. Lett.* 6 (2004) 1987.
- [38] R. Akiyama, T. Sagae, M. Sugiura, S. Kobayashi, *J. Organomet. Chem.* 689 (2004) 3806.
- [39] H. Miyamura, R. Akiyama, T. Ishida, R. Matsubara, M. Takeuchi, S. Kobayashi, *Tetrahedron* 61 (2005) 12177.
- [40] I.R. Cohen, T.C. Purcell, A.P. Altshuller, *Environ. Sci. Technol.* 1 (1967) 247.
- [41] R. Burch, P.R. Ellis, *Appl. Catal. B* 42 (2003) 203.
- [42] G. Bercic, A. Pintar, *Chem. Eng. Sci.* 52 (1997) 3709.